NASA/TM—2017–219844

Multilayer Insulation Ascent Venting Model

R.W. Tramel
Kord Technologies, Inc., Huntsville, Alabama

S.G. Sutherlin
Marshall Space Flight Center, Huntsville, Alabama

W.L. Johnson
Glenn Research Center, Cleveland, Ohio

December 2017

The NASA STI Program…in Profile

Since its founding, NASA has been dedicated to the advancement of aeronautics and space science. The NASA Scientific and Technical Information (STI) Program Office plays a key part in helping NASA maintain this important role.

The NASA STI Program Office is operated by Langley Research Center, the lead center for NASA's scientific and technical information. The NASA STI Program Office provides access to the NASA STI Database, the largest collection of aeronautical and space science STI in the world. The Program Office is also NASA's institutional mechanism for disseminating the results of its research and development activities. These results are published by NASA in the NASA STI Report Series, which includes the following report types:

- TECHNICAL PUBLICATION. Reports of completed research or a major significant phase of research that present the results of NASA programs and include extensive data or theoretical analysis. Includes compilations of significant scientific and technical data and information deemed to be of continuing reference value. NASA's counterpart of peer-reviewed formal professional papers but has less stringent limitations on manuscript length and extent of graphic presentations.

- TECHNICAL MEMORANDUM. Scientific and technical findings that are preliminary or of specialized interest, e.g., quick release reports, working papers, and bibliographies that contain minimal annotation. Does not contain extensive analysis.

- CONTRACTOR REPORT. Scientific and technical findings by NASA-sponsored contractors and grantees.

- CONFERENCE PUBLICATION. Collected papers from scientific and technical conferences, symposia, seminars, or other meetings sponsored or cosponsored by NASA.

- SPECIAL PUBLICATION. Scientific, technical, or historical information from NASA programs, projects, and mission, often concerned with subjects having substantial public interest.

- TECHNICAL TRANSLATION. English-language translations of foreign scientific and technical material pertinent to NASA's mission.

Specialized services that complement the STI Program Office's diverse offerings include creating custom thesauri, building customized databases, organizing and publishing research results…even providing videos.

For more information about the NASA STI Program Office, see the following:

- Access the NASA STI program home page at <http://www.sti.nasa.gov>

- E-mail your question via the Internet to <help@sti.nasa.gov>

- Phone the NASA STI Help Desk at 757–864–9658

- Write to:
  NASA STI Information Desk
  Mail Stop 148
  NASA Langley Research Center
  Hampton, VA 23681–2199, USA

NASA/TM—2017–219844

Multilayer Insulation Ascent Venting Model

R.W. Tramel
Kord Technologies, Inc., Huntsville, Alabama

S.G. Sutherlin
Marshall Space Flight Center, Huntsville, Alabama

W.L. Johnson
Glenn Research Center, Cleveland, Ohio

National Aeronautics and
Space Administration

Marshall Space Flight Center • Huntsville, Alabama 35812

December 2017

TRADEMARKS

Available from:

NASA STI Information Desk
Mail Stop 148
NASA Langley Research Center
Hampton, VA 23681–2199, USA
757–864–9658

This report is also available in electronic form at
<http://www.sti.nasa.gov>

TABLE OF CONTENTS

LIST OF FIGURES

LIST OF FIGURES (Continued)

LIST OF TABLES

LIST OF ACRONYMS AND SYMBOLS

ASME	American Society of Mechanical Engineers
CBT	cold boundary temperature
GN_2	gaseous nitrogen
KSC	Kennedy Space Center
LH_2	liquid hydrogen
LN_2	liquid nitrogen
MHTB	multipurpose hydrogen test bed
MLI	multilayer insulation
N_2	nitrogen
OML	outer mold line
SOFI	spray-on foam insulation
TM	Technical Memorandum
TVS	thermodynamic vent system
VC	vacuum can
VCR	vacuum coupling radiation
VD	variable density
WBT	warm boundary temperature

NOMENCLATURE

A	area
C	particle velocity
C_p	specific heat with constant pressure, J/kg/K
C_v	specific heat with constant volume, J/kg/K
d_p	diameter of pores in the MLI
g_c	dimensional constant
h_{fg}	heat of vaporization
k	Boltzmann constant
M	Mach number
m	mass
$\dot{m}$	mass flow rate
P	pressure, Pa
Q, q	heating rate; heat flux, W/m^2
$\dot{Q}$	heating rate
R	specific gas constant
T	temperature
TW	temperature of layers within MLI
t	time, hr
α	empirical constant
γ	specific heat ratio

NOMENCLATURE (Continued)

ε	emissivity
κ	thermal conductivity
λ	mean free path
ρ	density, kg/m^3
σ	Stefan-Boltzmann constant, $W/(m^2 \cdot K^4)$

TECHNICAL MEMORANDUM

MULTILAYER INSULATION ASCENT VENTING MODEL

1. INTRODUCTION

This Technical Memorandum (TM) describes the multilayer insulation (MLI) ascent venting model, a new predictive mathematical modeling capability allowing estimation of the thermal and venting performance of flight cryogenic storage tank MLI systems.

Future space missions will include vehicles using chemical or nuclear thermal propulsion. These propulsion technologies utilize liquid hydrogen (LH_2), liquid oxygen, and liquid methane as propellants. These cryogens must be stored beginning at Earth launch and throughout flight until needed for engine operation. Storage times will vary from several hours to many months, depending on when propulsion is required.

During a typical space flight, the cryogen storage tanks will be subjected to warm and cold environments. Most of these environments are warmer than the cryogenic propellants, so the resulting environmental heat loads must be removed from the stored liquids or intercepted before they reach the stored liquids in order to reduce or eliminate propellant losses. The tank insulation system helps by deflecting a portion of the environmental heat loads.

Detailed knowledge of expected performance of cryogenic propellant storage tank MLI is essential for the development of efficient tank insulation designs and accurate estimation of cryogenic propellant quantities for flight. Excellent predictive tools are available for application to orbital and transit environments and such heat loads are well understood.

The thermal and venting transient experienced by tank-applied MLI in the Earth-to-orbit environment is very dynamic and not well characterized. Until now, an accurate and reliable predictive tool for this problem has been lacking. A new approach has been taken with the development of the MLI ascent venting model. This new predictive code is a first principles-based engineering model that tracks the time history of the mass and temperature (internal energy) of the gas in each MLI layer. A continuum-based model is used for early portions of the trajectory while a kinetic theory-based model is used for the later portions of the trajectory, and the models are blended based on a reference mean free path λ_r. This should improve understanding of the Earth-to-orbit transient and enable better insulation system designs for in-space cryogenic propellant systems.

2. CODE OVERVIEW

2.1 Problem Setup

The overall schematic of the modeled system is displayed in figures 1 and 2. Here, there is a system of MLI blankets surrounding a tank of cryogen in either a ground test facility or a launch vehicle. The tank may be surrounded with spray-on foam insulation (SOFI). The pressure surrounding the tank is reduced to near vacuum levels by either a flight trajectory or a facility pump down profile. The current code tracks the thermodynamic state of the gas in the layers between the MLI and the heat transfer into the tank. The layers transfer energy from the warm boundary into the tank, and gas escapes from the MLI as the external pressure drops.

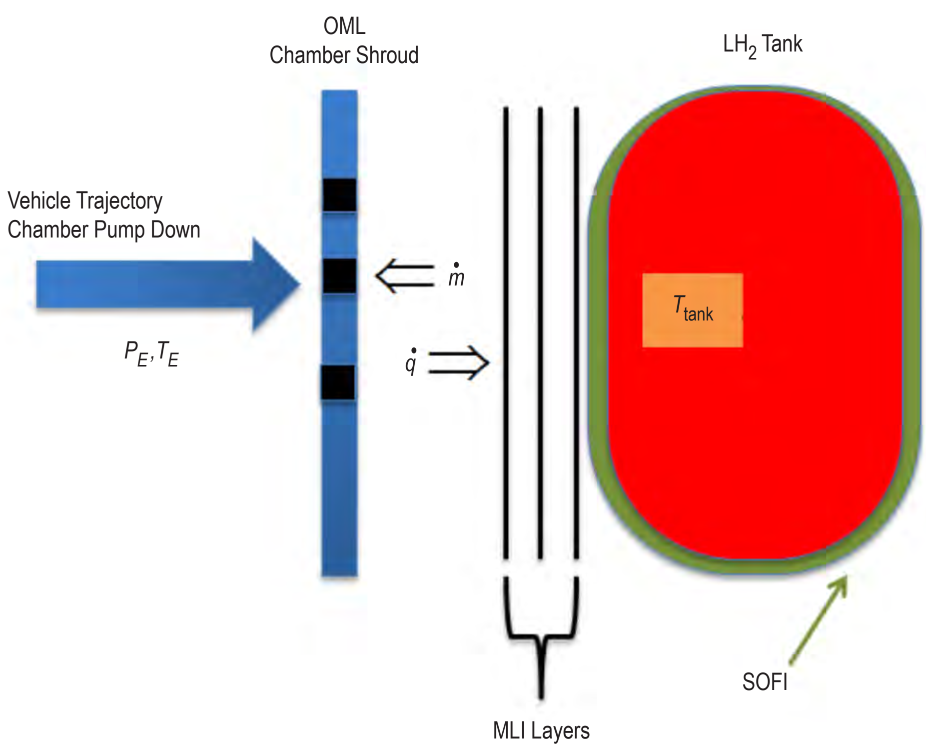

Figure 1. MLI heat transfer setup.

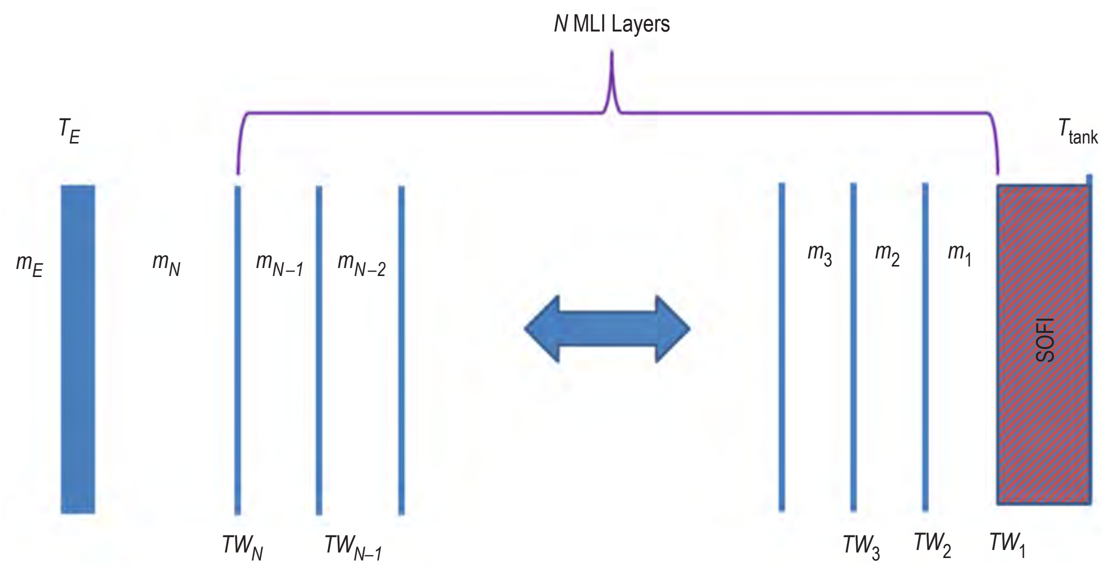

Figure 2. Mathematical model schematic.

The basic variables in the model are the temperatures of each of the layers in the MLI (TW_i) and the mass trapped between each layer (m_i). All properties of the gas in layer i requiring temperature are evaluated using the average of the neighboring wall temperatures: $0.5 \times (TW_i + TW_{i+1})$. It is assumed that the area variation between layers is small enough that geometrical considerations can be ignored and a unit-sized planar area is adopted. Each of the layers has a given porosity, and the porosity of the outer mold line (OML) and shroud may be different from those of the layers. Variable locations are shown in figure 2.

2.2 Mass Transfer Model

As the pressure external to the MLI drops from near atmospheric pressure at the start of a launch or test down to near vacuum conditions, the residual gas trapped between the MLI layers will migrate out of the MLI. A continuum-based model for the mass per time ($\dot{m}_i$) flowing from layer to layer is used for early portions of the trajectory while a kinetic theory-based model is used for the later portions of the trajectory, and the models are blended based on a reference mean free path $\lambda_r = d_p$, where d_p is the typical diameter of the pores in the MLI:

$$\dot{m}_i = f\left(\lambda,\lambda_r\right)\dot{m}_k + \left(1 - f\left(\lambda,\lambda_r\right)\right)\dot{m}_c \quad . \tag{1}$$

A plot of the proposed blending function is shown in figure 3.

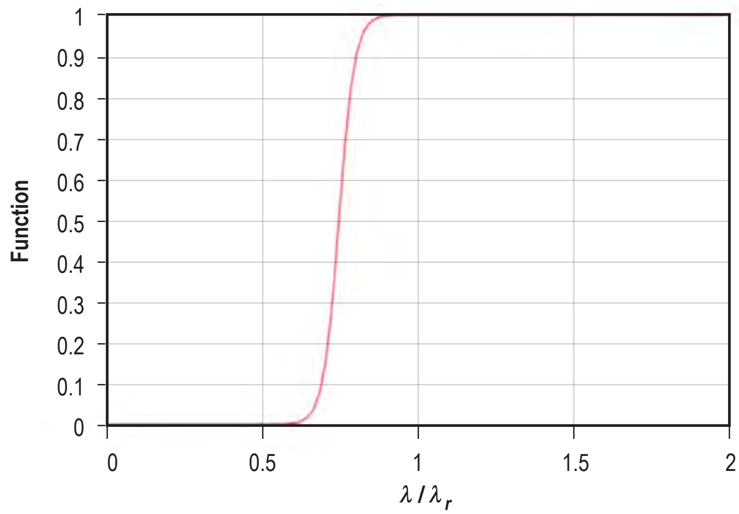

Figure 3. Proposed blending function.

2.2.1 Kinetic Theory-Based Mass Transfer Model

The kinetic theory model is based on the assumption that the distribution of particle velocities in each volume is given by a Maxwellian distribution, i.e., the probability of finding a particle with velocity between C_x, C_y, C_z and $C_x + dC_x$, $C_y + dC_y$, $C_z + dC_z$ is given by:[1]

$$f\left(C_x, C_y, C_z\right) = \frac{a^{3/2}}{\pi^{3/2}} e^{-a\left(C_x^2 + C_y^2 + C_z^2\right)} \quad , \tag{2}$$

where

a = $m/2kT$
m = mass of 1 molecule
k = Boltzmann constant
T = temperature.

The differential mass flux out of volume i into volume $i+1$ can be derived from the Maxwell distribution function as follows:

$$\frac{dm_i}{dt} = -A_{i,i+1} \frac{a^{3/2}}{\pi^{3/2}} \int_{-\infty}^{+\infty} \int_{-\infty}^{+\infty} \int_{0}^{+\infty} \left(\rho_i C_x f\left(C_x, C_y, C_z\right)\right) dC_x \, dC_y \, dC_z \quad , \tag{3}$$

which can be evaluated to yield

$$\frac{dm_i}{dt} = -A_{i,i+1} \rho_i \frac{\bar{C}_i}{4} \quad , \tag{4}$$

where $\bar{C}_i = \frac{2}{\pi^{1/2}}\left(\frac{2kT_i}{m}\right)^{1/2}$ is the average particle speed in volume i. The kinetic theory mass flux equation is written in general as:

$$\frac{dm_i}{dt} = -A_{i,i+1}\left(\frac{\rho_{i+1}\bar{C}_{i+1}}{4} - \frac{\rho_i\bar{C}_i}{4}\right) + A_{i,i-1}\left(\frac{\rho_{i-1}\bar{C}_{i-1}}{4} - \frac{\rho_i\bar{C}_i}{4}\right) \quad . \tag{5}$$

2.2.2 Continuum-Based Mass Transfer Model

The continuum-based model begins with the exact formula for the mass flow through an orifice of area A which has been expanded to a Mach number M from stagnation conditions P_t and T_t:[2]

$$\frac{\dot{m}}{A} = M\left(1 + \frac{\gamma - 1}{2}M^2\right)^{-(\gamma+1)/2(\gamma-1)}\left(\frac{\gamma g_c}{R}\right)^{1/2}\frac{P_t}{\sqrt{T_t}} \quad . \tag{6}$$

This equation was used as a basis for a model in which the Mach number M was determined by isentropically expanding the gas such that the dynamic pressure of the flow coming through the orifice was matched to the static pressure on the low pressure side of the orifice. However, a simpler approach was adopted in which the mass flow from volume i to volume $i+1$ is given by:

$$\dot{m}_{i,i+1} \approx \alpha A\left(\frac{P_{i+1}}{\sqrt{T_{i+1}}} - \frac{P_i}{\sqrt{T_i}}\right) \; , \tag{7}$$

where α is determined from numerical experiments. This formulation was found to behave better on large systems of equations. A comparison of the two approaches on a simple Joule-Thomson expansion is shown in figure 4.

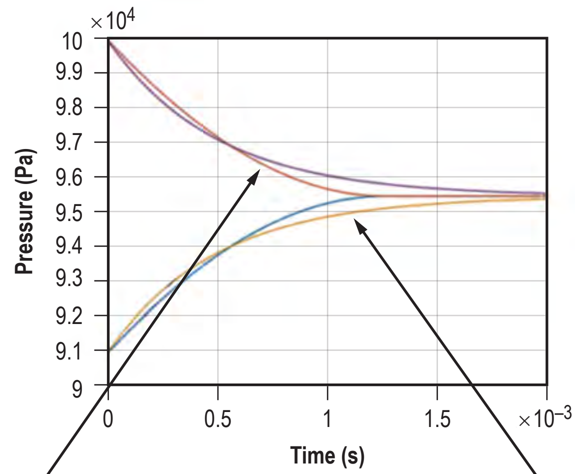

$$\frac{\dot{m}}{A} = M\left(1+\frac{\gamma-1}{2}M^2\right)^{-(\gamma+1)/2(\gamma-1)}\left(\frac{\gamma g_c}{R}\right)^{1/2}\frac{P_t}{\sqrt{T_t}}$$

$$\dot{m}_{i,i+1} \approx \alpha A\left(\frac{P_{i+1}}{\sqrt{T_{i+1}}}-\frac{P_i}{\sqrt{T_i}}\right)$$

Figure 4. Continuum-based mass transfer model applied to Joule-Thompson expansion.

2.2.3 Seam Strategy

Often the MLI blankets are applied around the tank in a set of discrete layers. As a first attempt at developing a model for this situation, consider the diagram shown in figure 5. In this situation, the pressures within each group of blankets are equalized by coupling the mean pressure in each group ($\bar{P}_i$) to P_{ext} using the following equation:

$$\dot{m}_{i,\text{seam}} \approx \alpha_{\text{seam}} A_{\text{seam}}\left(\frac{P_{\text{ext}}}{\sqrt{T_{\text{ext}}}}-\frac{\bar{P}_i}{\sqrt{T_i}}\right) . \tag{8}$$

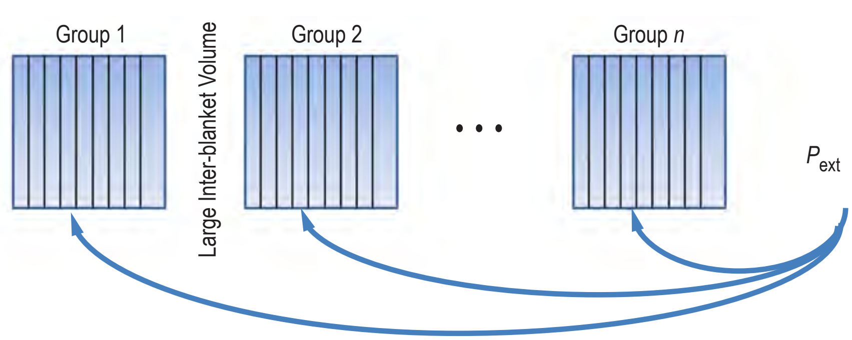

Figure 5. Blanket seam strategy.

For pressure drop rates typical of launch profiles, $\alpha_{\text{seam}} = \alpha \approx 0.005$ is set.

2.3 Coupled Thermal Solver

In this effort the researchers chose to develop a model for the temperatures of the MLI layers and to assume that the temperature of the gas between these layers is the average of the neighboring wall temperatures. The general time evolution equation for an interior layer follows:

$$M_i C_p \frac{TW_i}{dt} = \frac{\kappa_i}{dr_i}\left(TW_{i+1} - TW_i\right) + \frac{k_{i-1}}{dr_{i-1}}\left(TW_{i-1} - TW_i\right)$$

$$+ \frac{\sigma}{\frac{1}{\varepsilon_{i+1}} + \frac{1}{\varepsilon_i} - 1}\left(TW_{i+1}^4 - TW_i^4\right) + \frac{\sigma}{\frac{1}{\varepsilon_{i+1}} + \frac{1}{\varepsilon_i} - 1}\left(TW_{i-1}^4 - TW_i^4\right) \;, \quad (9)$$

where σ is the Stefan-Boltzmann constant. For layer 1 $TW_0 = T_{\text{tank}}$ is set, and if a layer of SOFI is present the conductivity of the gas κ_0 is replaced by κ_{SOFI} and $dr_0 = dr_{\text{SOFI}}$ while $TW_{N+1} = T_{\text{ext}}$ is set for layer N.

The coupling of the thermal model to the mass transfer term model comes through gas conductivities (κ). A kinetic theory-based approximation is used in the simplest model:[3]

$$\kappa_i = \frac{9\gamma - 5}{8}\rho_i C_v \bar{C}_i \min\left(\lambda_i, dr_i\right) \;. \quad (10)$$

In this simple model, the conductivity of the gas is independent of the pressure until the mean free path in gas layer i becomes greater than the spacing. At this point, the conductivity decays with particle density and the model switches seamlessly from the continuum to a free molecular approach.

3. TEST CASES

The new code has been applied to the A125 test at NASA Kennedy Space Center (KSC) and to the multipurpose hydrogen test bed (MHTB) test series at NASA Marshall Space Flight Center.

3.1 A125 Test Article

The A125 test was conducted at KSC using the Cryostat-100.[4] The description of the test setup is taken from reference 4 (figures 1 and 2 mentioned here correspond to figures 6 and 7 in this TM):

> [The Cryostat-100] is guarded on top and bottom for absolute thermal performance measurement. The basic schematic and a photograph of the overall arrangement, including the mechanical lift mechanism, are shown in figure 1. A cold mass assembly, including the top and bottom guard chambers and a middle test chamber, is suspended from a domed lid atop the vacuum canister, as shown in figure 2.
>
> Each of the three chambers is filled and vented through a single feedthrough (also connected from the lid) for easy operation and minimum overall heat leakage... All fluid and instrumentation feedthroughs are mounted and suspended from a top-domed lid for easy removal of the cold mass.
>
> Cryostat-100 includes an external heating system for bakeout and high heat load tests, as well as an internal heater system for fine control of the warm boundary temperature (WBT). Three custom-designed funnel filling tubes (7.93-mm outside diameter) interface with the three LN2 feedthroughs (12.7-mm outside diameter) and provide the means for cooldown, filling, and replenishment by pouring from a small nonpressurized dewar. The filling tubes are removed when not being used. Connected to the top ports of the LN2 feedthroughs are the plastic tubing assemblies that route the boiloff flow from all three liquid chambers to their respective mass flow meters.... The vacuum pumping system includes a directly connected turbopump and a separately plumbed mechanical pump. In addition, a gaseous nitrogen (GN2) supply system provides purging and residual gas pressure control to vacuum levels as low at $5 \times 10-5$ torr.
>
> ...A custom lift mechanism, shown in figure 1, allows the cold mass assembly and insulation test specimen to be manipulated easily. The location of temperature feedthroughs on the lid allows the sensors to move with the cold mass assembly when insulation specimens are installed.

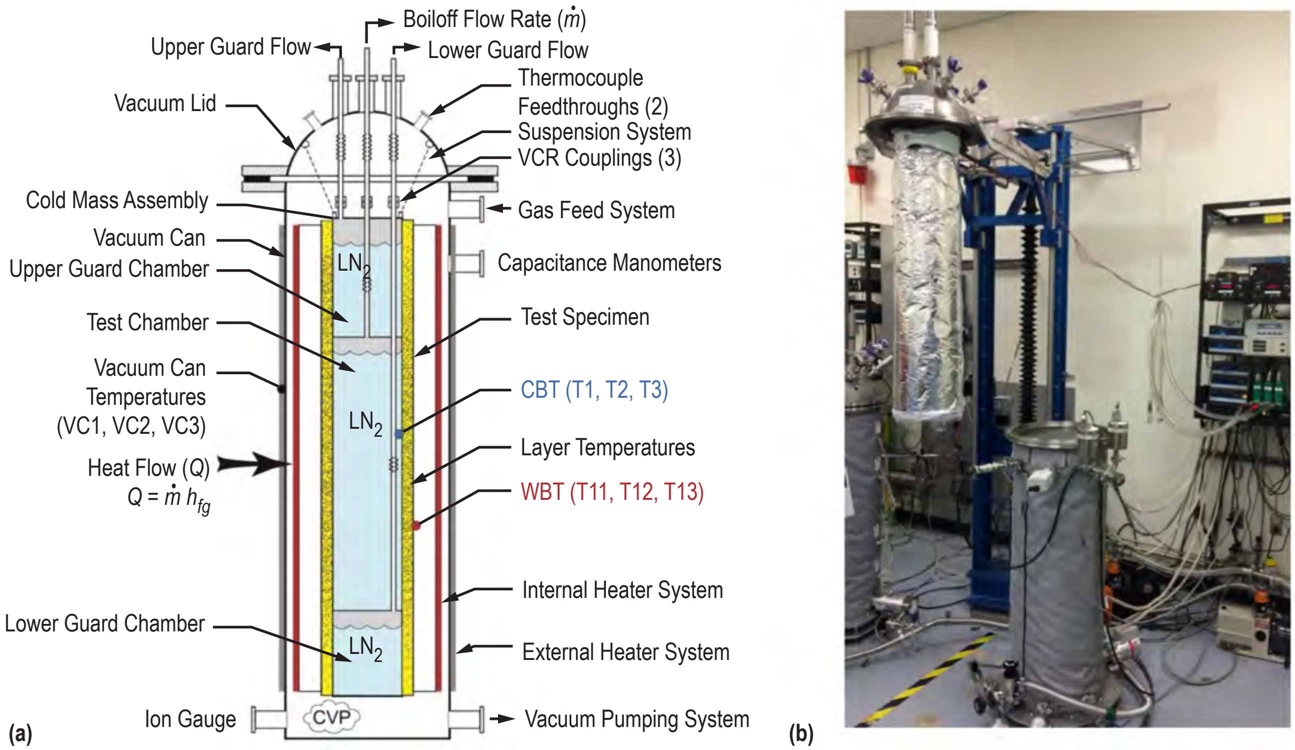

Figure 6. Cryostat-100: (a) Basic schematic and (b) overall arrangement with lift mechanism.

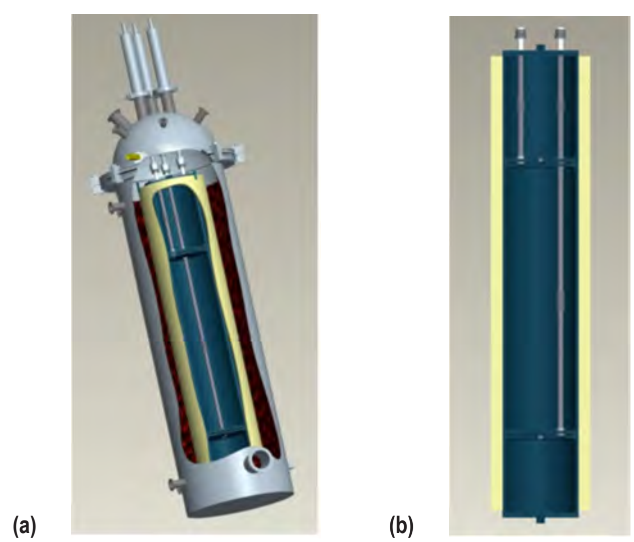

Figure 7. Simplified views of Cryostat-100: (a) Overall system and (b) cold mass assembly.

3.1.1 A125 Test Results

The A125 test article is a 40-layer, 16-mm-thick DuPont Mylar® net MLI configuration. Properties of the MLI are shown in table 1. A simulation has been been performed for this configuration. A schematic of temperature probe locations is shown in figure 8. Plots of the cold and warm boundary temperature probes T2 and T12 versus time are shown in figure 9. A comparison of the measured and computed heat transfer rates is shown in figure 10. In general, the comparison between the heat transfer rates is good, although the predicted rate shows a departure from the measured values between 200 and 500 min. A comparision of the vaccum chamber pressures shown in figure 11 also indicates a rise and fall in the vaccum chamber pressure. Since gas conduction is still the dominate heat transfer rate in this regime, it is argued that if this pressure departure were real, then it would have resulted in increased heat transfer. In order to investigate this possibility, a monotonically decaying pressure profile was constructed and the simulation was rerun. The results, shown in figures 12 and 13, demonstrate the improvement in agreement. Finally, temperature distriubutions within the MLI at the beginning and the end of the test are shown in figures 14 and 15.

Table 1. A125 properties.

Mass per layer (kg)	0.013
C_p (J/kg/K)	4,187
MLI emissivity*	$0.0035T^{1/2}$
Tank emissivity*	0.12
Estimated gap between tank and MLI (m)	0.001

* See reference 5.

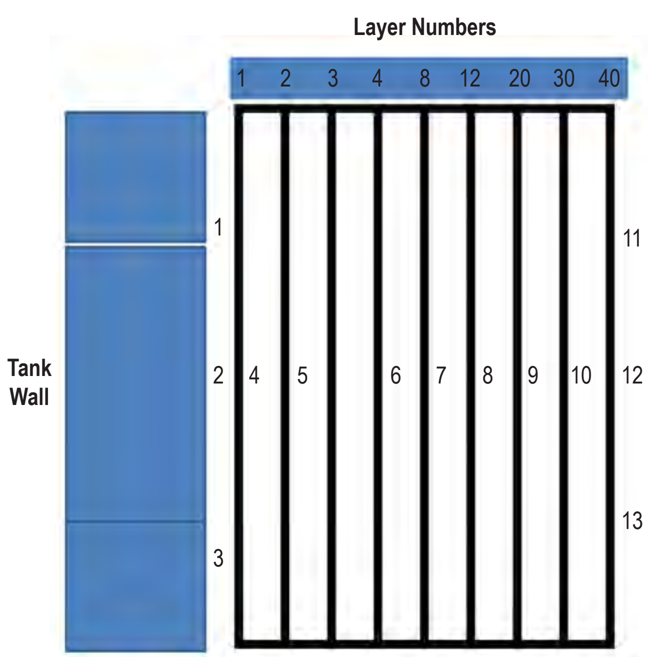

Figure 8. A125 temperature probe locations.

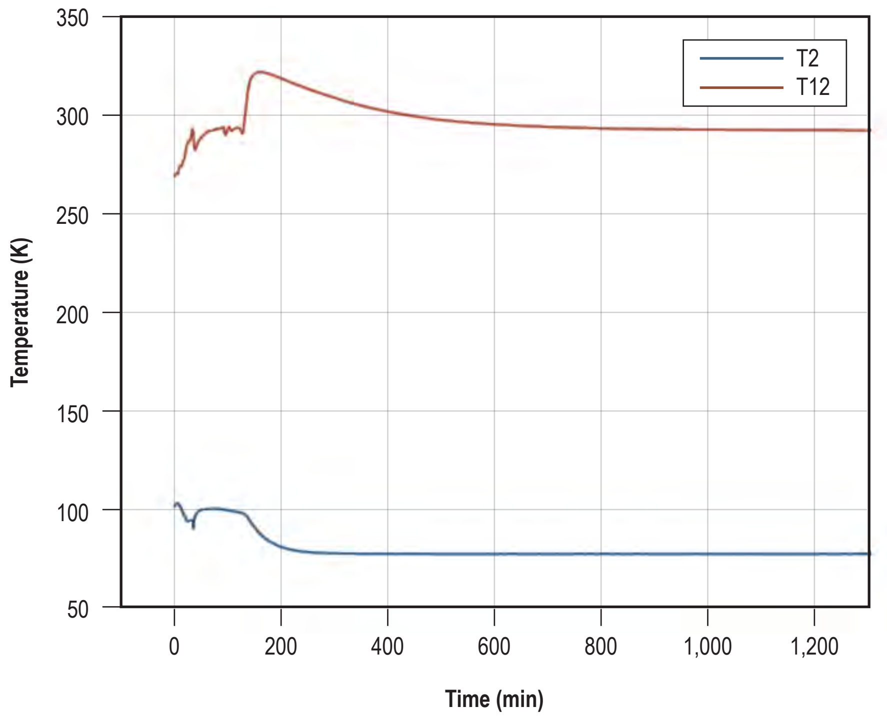

Figure 9. Warm and cold boundary temperatures (T2 and T12) in A125 test.

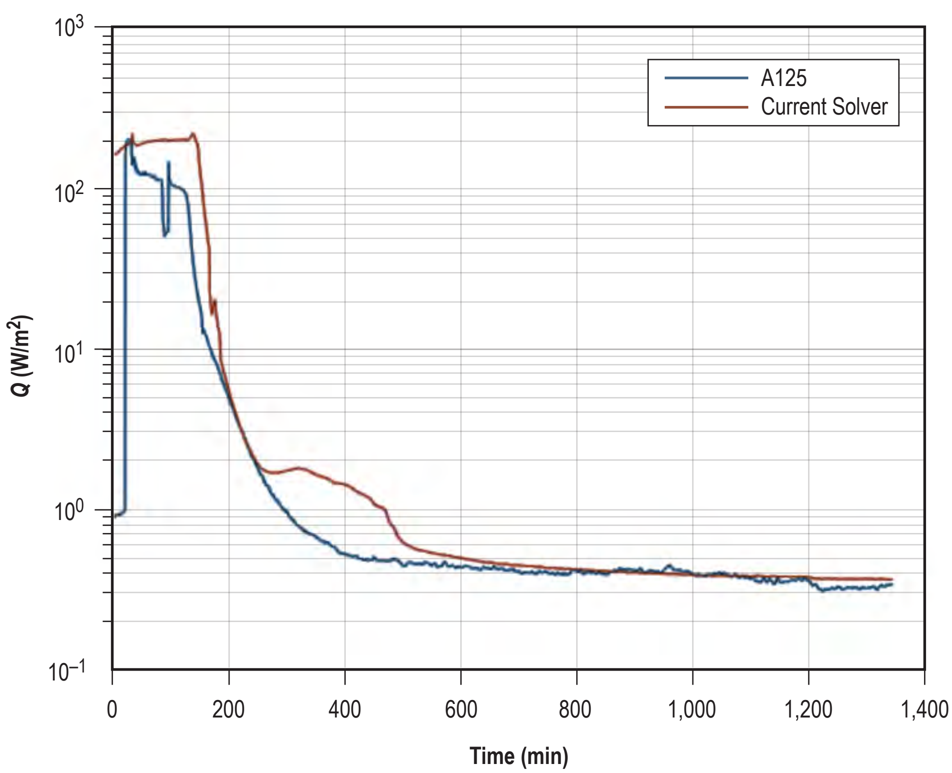

Figure 10. $\dot{Q}$ comparison of measured and predicted heat transfer rates in A125 test.

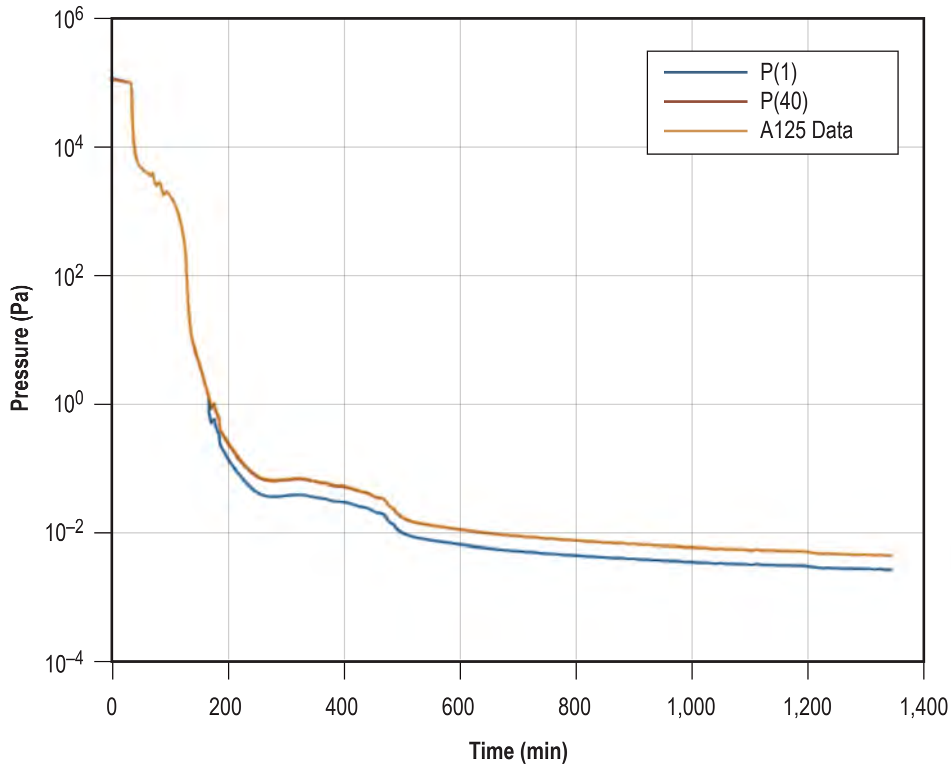

Figure 11. Comparison of pressures in the MLI in A125 test.

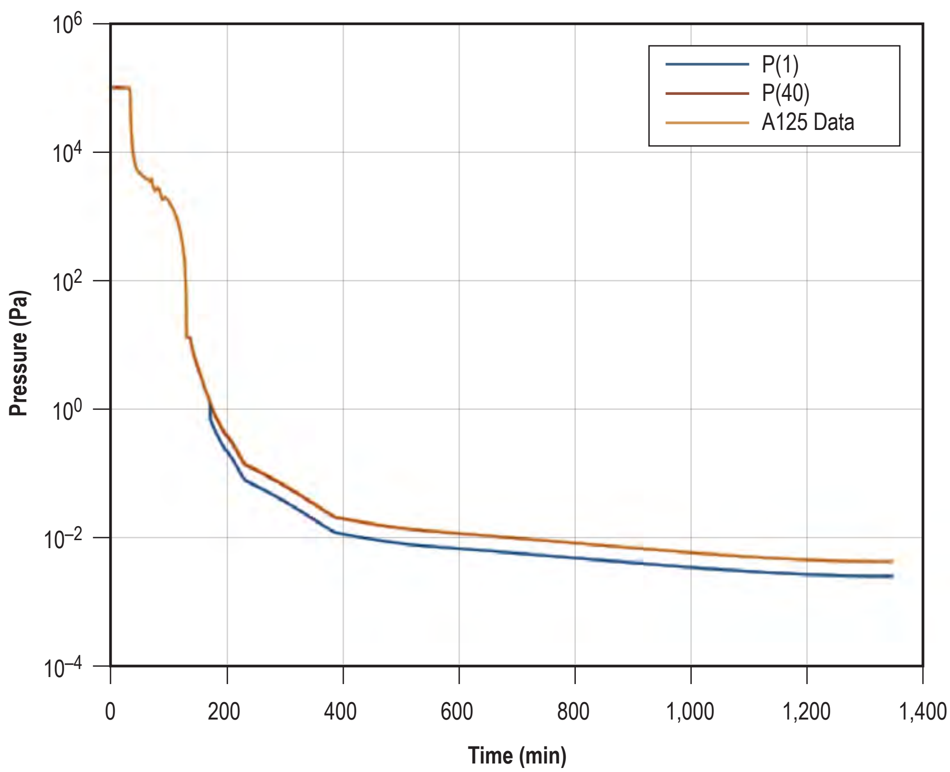

Figure 12. Monotonically decaying pressure profile in A125 test (smooth pressure profile).

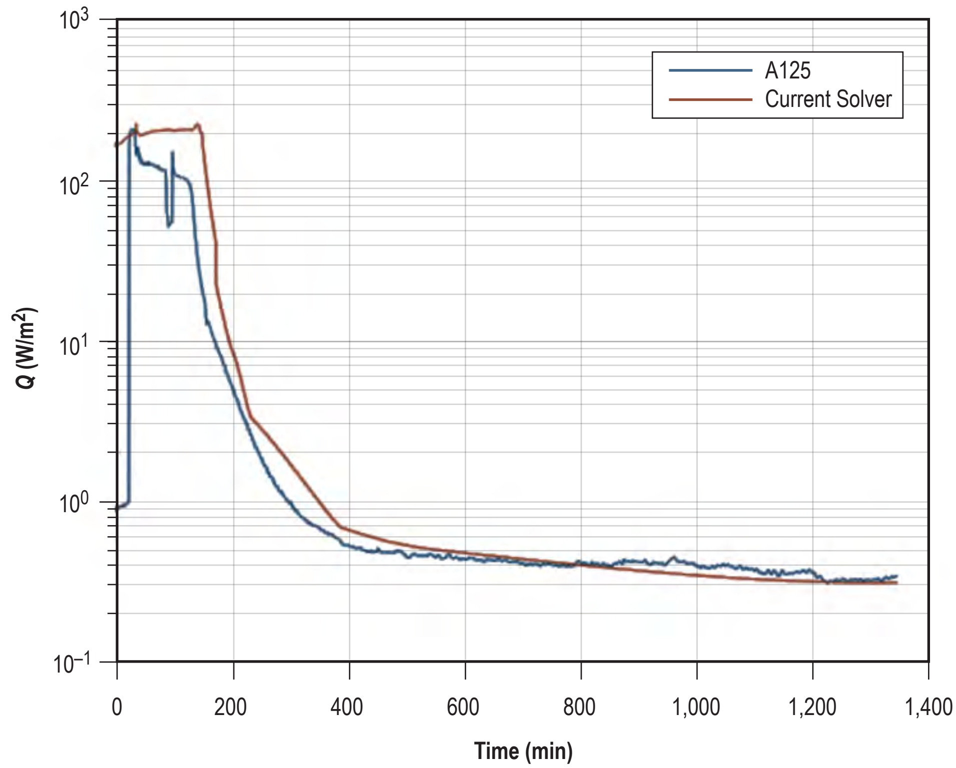

Figure 13. Q comparison of measured and predicted heat transfer rates in A125 test (smooth profile).

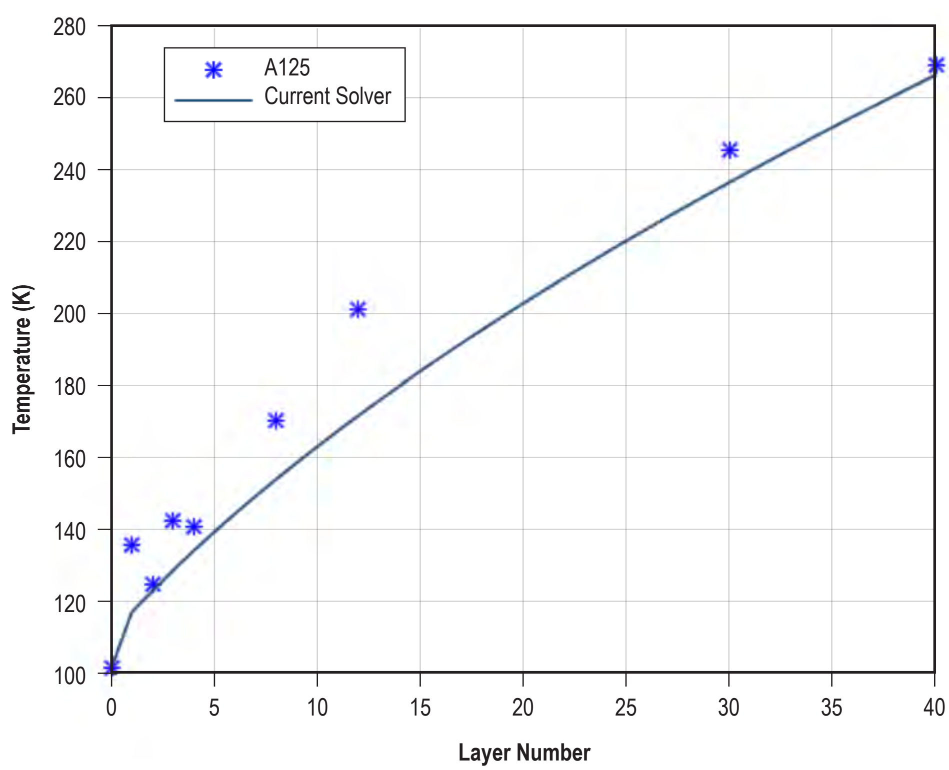

Figure 14. Comparison of MLI temperature distributions at T = 0 hr in A125 test.

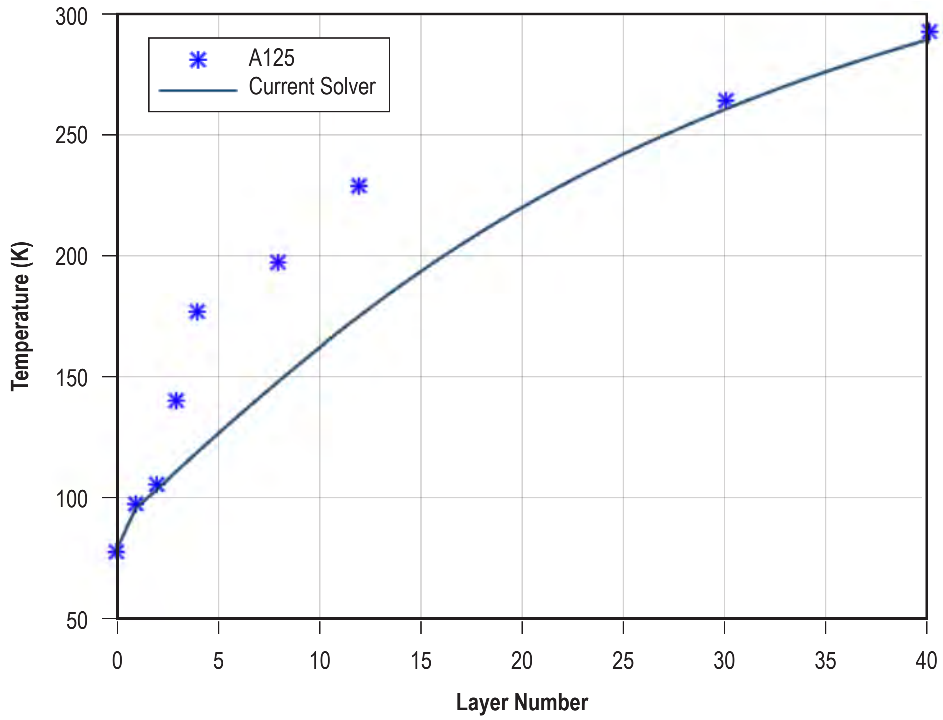

Figure 15. Comparison of MLI temperature distributions at T = 22 hr in A125 test.

3.2 Multipurpose Hydrogen Test Bed Test Article

The major test article elements consist of the MHTB tank, an environmental shroud, a cryogenic insulation subsystem, and test article instrumentation. Technical descriptions of each of these elements are summarized below, with further details presented in reference 6.

3.2.1 Multipurpose Hydrogen Test Bed Tank

The MHTB 5083 aluminum tank is cylindrical in shape with both a height and diameter of 3.05 m and 2:1 elliptical domes as shown in figure 16. The tank has an internal volume of 18.09 m^3 and a surface area of 34.75 m^2. The tank is ASME pressure vessel-coded for a maximum operational pressure of 344 kPa and was designed to accommodate various cryogenic fluid management technology and advanced concepts as updated versions become available. More details on the test article may be found in reference 5.

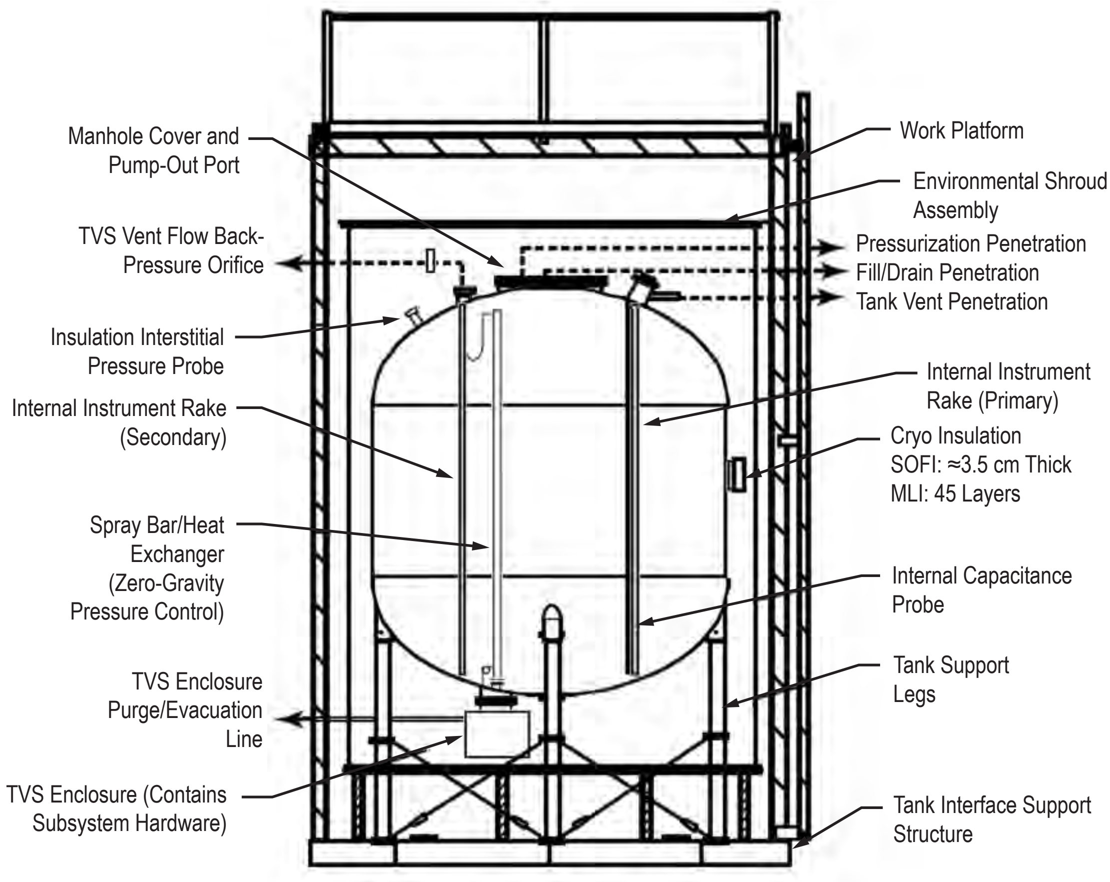

Figure 16. MHTB test tank and supporting hardware schematic.

3.2.2 Environmental Shroud

The MHTB tank is enclosed within an environmental shroud that simulates a ground hold conditioning purge, similar to that in a payload bay, and enables the imposition of a range of uniform temperatures on the MLI external surfaces. Seen in figure 17, the shroud is 4.57 m high and 3.65 m in diameter, and contains a purge ring for distributing dry N_2. The shroud heater strips and cooling loops can impose either constant or time-dependent boundary temperatures ranging from 80 to 320 K on the MHTB exterior surfaces.

Figure 17. MHTB environmental shroud assembly.

3.2.3 Cryogenic Insulation Subsystem

The MHTB insulation concept consists of a combination of foam and variable density- (VD-) MLI. During ground hold and ascent flight the foam element enables a GN_2 purge, as opposed to a helium purge, and reduces heat leak. The SOFI, termed Isofoam SS–1171, was applied directly to the tank surface with a robotic process at a thickness of 3.18 ± 0.63 cm which was the minimum that could be applied with available equipment and procedures at the time. An average thickness of 3.53 cm (1.4 in) was calculated based on measurements with a Kaman© eddy current device.

A 45-layer VD-MLI blanket placed over the SOFI provides thermal protection while at vacuum or orbital conditions. Unique features of the VD-MLI concept include utilization of a variable density (layers-per-unit thickness) concept for radiation shields to provide a more weight-efficient insulation system and the use of fewer but larger perforations for venting during ascent to orbit. As illustrated in figure 18, the variable density was accomplished using bumper strips of variable thickness to provide more layers in warmer regions (16 layers/cm on outside segment), and fewer layers in the colder region where radiation blockage is less important (8 layers/cm). The layup resulted in an estimated average layer density of 12 layers/cm (30 layers/in). The vent hole perforation pattern, which provides a 2% open area, is unusual in that the perforation size is large (1.27 cm (0.5 in) in diameter) and the holes are more widely spaced (7.6 cm (3 in)). Standard perforations are 0.16 to 0.08 cm (0.063 to 0.031 in) in diameter with spacing of about 0.9 cm (0.37 in) and a +2%–4% open area. The larger holes reduce the radiation view factor—hence, the radiation exchange—between layers. Details of the MHTB insulation concept are summarized in table 2.

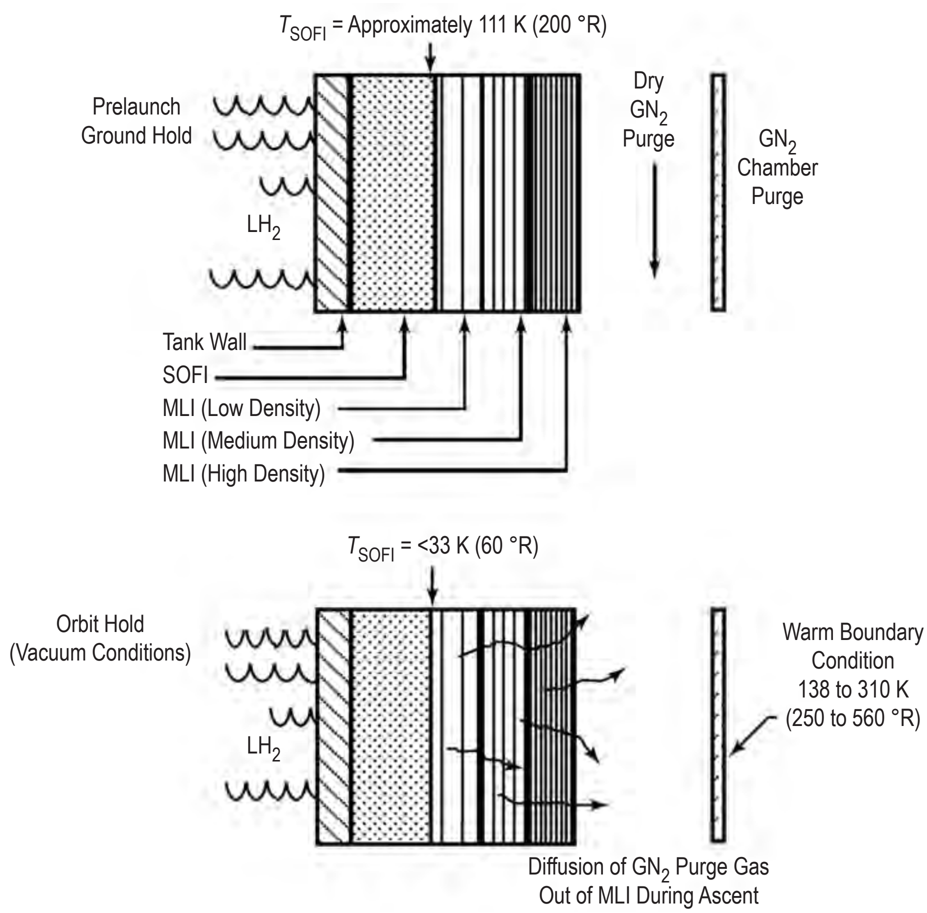

Figure 18. MHTB insulation concept using VD-MLI with foam substrate.

Table 2. MHTB properties.

Mass per layer (kg)	0.013
C_p (J/kg/K)	4,187
MLI emissivity	0.031
κ_{SOFI} (W/m/K)	0.000866
dr_0 (SOFI thickness, cm)	3.5
dr_i (average layer spacing, cm)	1/12
MLI porosity (%)	2

3.2.4 Multipurpose Hydrogen Test Bed Orbit Hold Comparisons

Results of the three orbit hold simulations are tabulated in table 3. The insulation heat leak ($\dot{Q}_{insul}$) ranged from 10.93 to 2.98 W (0.31 to 0.085 W/m^2) for warm boundaries ranging from 305 to 164 K, with and without penetration heat guards, and include some off-nominal conditions. The first test (P9502), conducted without heat guards, yielded heat leaks of 10.71 and 4.38 W with boundaries of 305 and 164 K, respectively. The second test (P9601) yielded lower heat leaks than in the first test, that is, 8.66 and 8.51 W without the heat guards and with the 305 K boundary. The lower heat leak observed in the second test might be the result of reduced outgassing, probably from the foam insulation. With the penetration heat guards activated, an even lower heat leak of 7.6 W (0.22 W/m^2) occurred with the 305 K boundary. Comparisons between $\dot{Q}$ values computed by the current solver and other attempts[7] at modeling the heat leaks are displayed in figure 19. The overall agreement is encouraging.

Table 3. Steady-state measured orbit hold performance.

	Test Conditions						Measured TCS Performance (W)							Insulation Heat Flux (W/m^2)
Test	Initial Conditions	Chamber Press (torr)	Inter-stitial Press (torr)	Heat	Heater Shroud Temp (K)	Ullage Range (%)	$\dot{Q}_{boiloff}$	$\dot{Q}_{vent}$	$\dot{Q}_{fill\ line}$	$\dot{Q}_{press\text{-}line}$	$\dot{Q}_{legs}$	$\dot{Q}_{others}$	$\dot{Q}_{insul}$	$\dot{Q}_{insul}/A_{tank}$
P9502	Vacuum chamber rapid evacuation to orbit conditions after completion of ground hold test	6×10^{-8}	–	Off	305	12–17	13.10	0.05	0.07	0.71	1.45	0.10	10.71	0.31
		9×10^{-8}	–	Off	164	17–21	5.34	0.04	0.03	0.36	0.49	0.03	4.38	0.13
P9601	Vacuum chamber rapid evacuation to orbit conditions after completion of ground hold test	2×10^{-7}	–	Off	305	25–30	11.07	0.05	0.13	0.70	1.40	0.11	8.66	0.25
		6×10^{-8}	–	On	305	25–30	7.89	–	0.03	–	0.13	0.10	7.64	0.22
		2×10^{-7}	–	Off	305	25–30	10.90	0.05	0.16	0.67	1.40	0.11	8.51	0.24
		9×10^{-8}	–	Off	164	30–35	3.90	0.05	0.07	0.29	0.48	0.02	2.98	0.086
P9602A	Vacuum chamber evacuated to 10^{-5} torr and test article vacuum conditioned prior to tanking of LH_2	5×10^{-8}	8×10^{-6}	Off	235	5–8	8.41	0.05	0.09	0.52	0.89	0.05	6.82	0.20
		4×10^{-8}	4×10^{-6}	On legs only	235	5–8	7.28	0.05	0.09	0.50	0.08	0.05	6.52	0.19
		4×10^{-8}	1×10^{-7}	Off	305	8–12	12.87	0.06	0.12	0.78	1.37	0.11	10.47	0.30
		4×10^{-8}	1×10^{-7}	On legs only	305	8–12	12.11	0.05	0.12	0.81	0.13	0.09	10.93	0.31

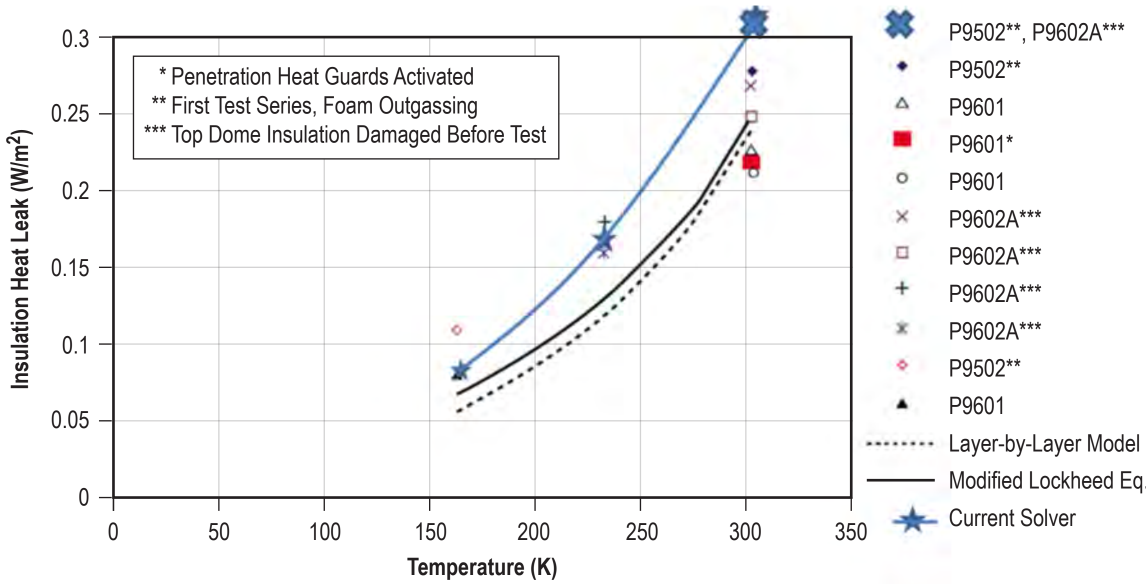

$$q = \left[\frac{2.4E - 4 * (0.017 + 7.0E - 6 * (800.0 - T_{avg}) + 2.28E - 2 * \ln(T_{avg}))(N^*)^{2.63} (T_h - T_c)}{nlayers} \right]$$

Note: For the current solver the solid conduction term from the modified Lockheed Eq. is added.

Figure 19. Comparison of MHTB orbit hold simulations.

3.2.5 Multipurpose Hydrogen Test Bed Ascent Simulation Comparisons

After a ground hold was completed during the P9502 simulations, a pressure pump down timeline similar to what would be experienced during an ascent profile was executed, and heat leak into the tank was measured. A comparison of the computed pressures and $\dot{Q}$s is shown in figures 20 and 21. As can be seen in figure 21, the predicted heat flux into the tank during ground hold was too high. This is likely due to temperature dependence of the SOFI and temperature. In order to explore the implications of this thought a little further, a curve fit was constructed which blended known values for SOFI conductivities with the values used during the orbit hold simulations. The shape of this curve fit is shown in figure 22. The simulation was rerun using these values and $\dot{Q}$ prediction obtained is displayed in figure 23. The comparison is much improved, but more data are needed on SOFI conductivities combined with high pressures and low temperatures before a definitive conclusion is reached. Also, with large temperature variations, the possibility remains that the SOFI will have to be discretized into a number of sub-blocks in order to accurately capture the flow of energy through the SOFI.

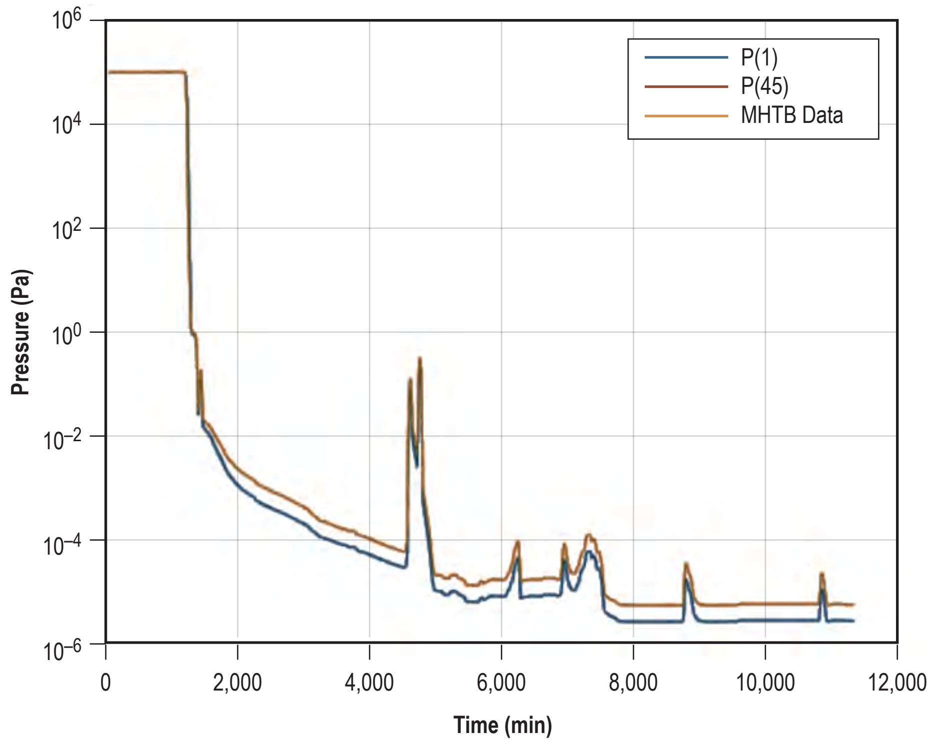

Figure 20. Pressure prediction comparison for MHTB ascent profile.

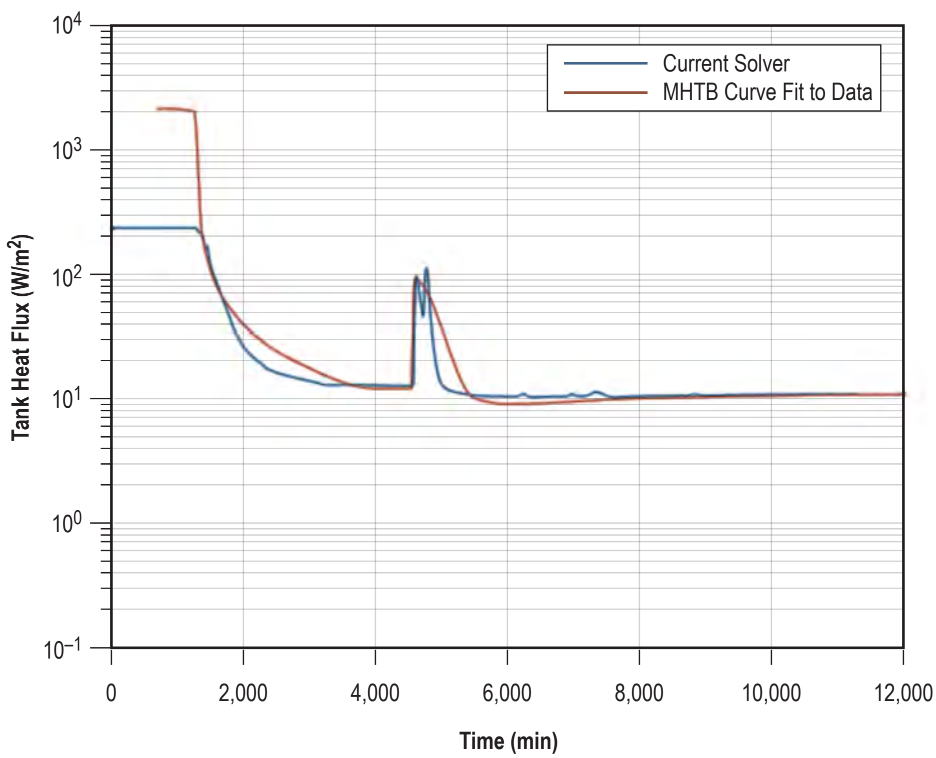

Figure 21. Heat flux prediction comparison for MHTB ascent profile.

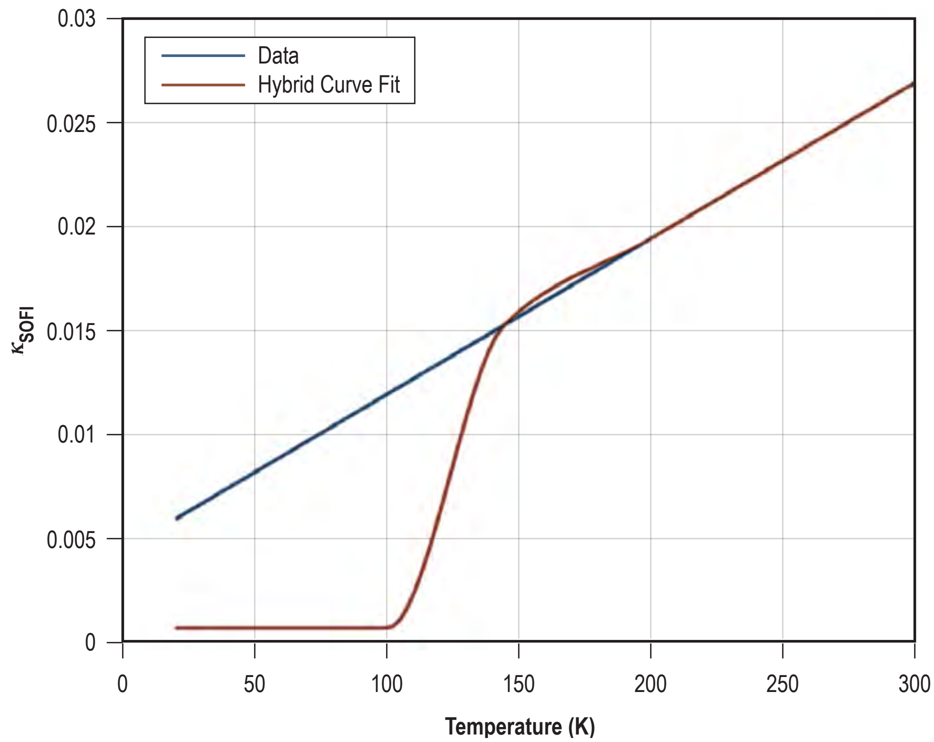

Figure 22. SOFI temperature-dependent conductivity.

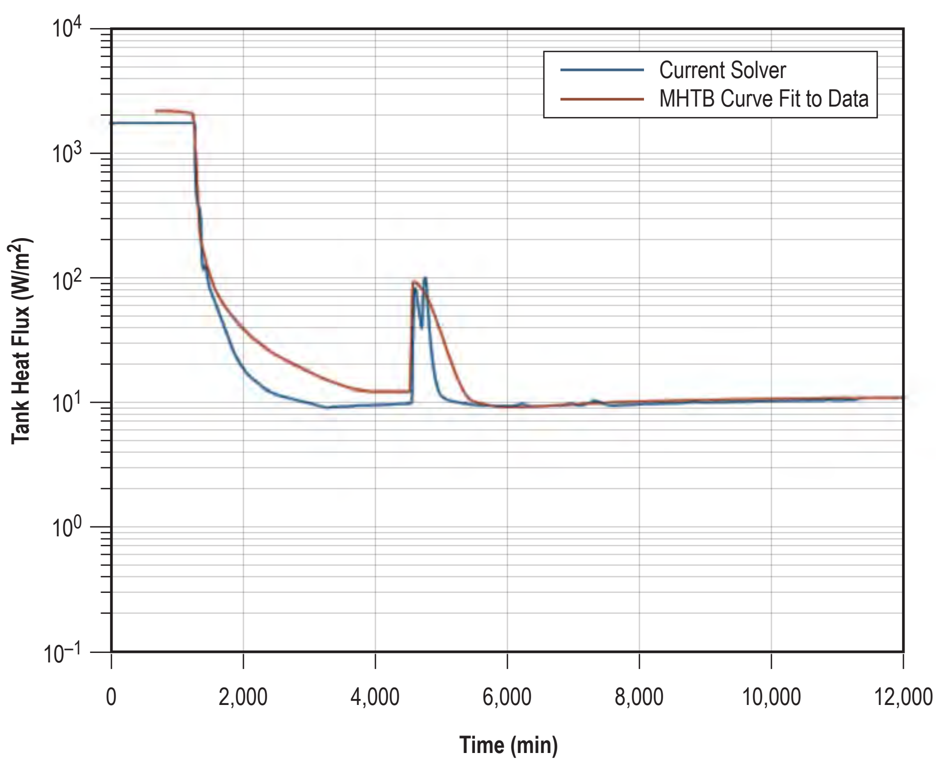

Figure 23. Heat flux prediction comparison for MHTB ascent profile.

4. USERS GUIDE

The equations in this TM have been coded into a MATLAB script. In order to use the script the user must first create the text file mlivalues.txt. A sample of this file is shown in table 4. Formats are %u for integers, %f for floating-point numbers, and %e for scientific notation.

Table 4. Values in mlivalues.txt file for A125 test.

Variable name	Format (%)	Values	Description
SOFI	u	–	1 if SOFI present, 0 otherwise
dr_sofi	f	0.00105	SOFI spacing (m)
rgas	f	297	Purge gas constant (N-m/kg/K)
Cp	f	1,055	Purge gas specific heat (J/kg/K)
d	e	3.80×10^{-10}	Molecular diameter
mol_weight	f	28.2	Molecular weight
porosity	f	2	MLI porosity (%)
dr	f	0.0004	MLI spacing (m)
nlayer	u	40	Number of layers
mass_per_layer	f	0.012928571	Mass per layer (kg/m^2)
cp_mli	f	4,187	MLI specific heat (J/kg/K)
mli_emissivity	f	0.031	MLI emissivity
tank_emissivity	f	0.13	Tanks emissivity
relax	f	–	Empirical constant (α)
ngroups	u	2	Number blanket groups
relax_seams	f	0.0004513	Empirical constant (α_{seams})
steady	u	1	1 to compute ground hold, 0 otherwise
ode	u	1	1 to compute ascent, 0 otherwise
restart	u	–	1 if this is a restart, 0 otherwise
deltat	f	80,588	Duration to perform ascent simulation (s)
nout	u	4,000	Number of output points

With this file one can run a ground test case, an ascent case, or both. The restart variable is necessary in order to interface with SINDA/FLUINT via a Fortran subroutine. In addition, if the external pressure or temperatures vary with time, the user needs to create MATLAB curve fits to the data such as pext_cf, tcb_cf, or twb_cf and store these in the MATLAB files pext_cf.mat, tcb_cf.mat, and twb_cf.mat. If any of these variables are constant, then the user needs to create the files pext.txt, tcb.txt, or twb.txt with the respective values placed in the files. The pressure should be in torr and temperatures in Kelvin. The MATLAB script will automatically generate a curve fit internally for use in these situations. An example of how to call the script from Fortran is displayed in the appendix. The user may modify this example to fit their needs.

4.1 Output

At present, the code writes out the temperature and pressure profiles in the MLI at the end of a simulation as well as the time history of the heat flux into the tank during the run into the files twall.txt, pgas.txt, and qt.txt for use by the user. Other outputs are easily added as needed.

5. CONCLUSION

A first principles-based tool for the prediction has been presented and compared to two different MLI configurations. In general, the agreement is encouraging, but more experimental work is needed to characterize the temperature, pressure dependence, and hysteresis effects on the conductivity of SOFI in order to remove uncertainty in the use of the model for hybrid SOFI/MLI configurations.

APPENDIX—SAMPLE FORTRAN DRIVER PROGRAM

```
program rmat
integer(kind=4) :: nlayer=40,nout=400
integer(kind=4) :: file01,file02,file03
real(kind=8)    :: tcb,twb,pext
real(kind=8)    :: twall(200),pgas(200),qtank(4000)
file01=1
file02=2
pext=772.3673 !Torr
tcb=101.7245  !Kelvin
twb=268.9604  !Kelvin
call call_mli(nlayer,nout,file01,file02,file03,tcb,twb,pext,twall,pgas,qtank)
write(6,*) twall(1),pgas(1),qtank(1)
end program rmat
!!!!!!!!!!!!!!!!!!!!!!!!!!!!!
subroutine call_mli(nlayer,nout,file01,file02, &
file03,tcb,twb,pext,twall,pgas,qtank)
integer(kind=4), intent(in)   :: nlayer,nout,file01,file02,file03
real(kind=8),    intent(in)                          :: tcb,twb,pext
real(kind=8),    intent(out), dimension(nlayer+2) :: twall
real(kind=8),    intent(out), dimension(nlayer)   :: pgas
real(kind=8),    intent(out), dimension(nout)     :: qtank
!!!!!!!!!!!!!!!!!!!!!!!!!!!!!!!!
!write values for time advance
open(file01,file='pext.txt')
write(file01,*) pext
close(file01)
!
open(file01,file='tcb.txt')
write(file01,*) tcb
!
close(file01)
open(file01,file='twb.txt')
write(file01,*) twb
close(file01)
!!!!!!!!!!!!!!!!!!!!!!!!!!!!!!!!!!!!!!!!!!!!!!!!
! run matlab from command line
call execute_command_line("matlab_2015b -noawt -nosplash -nodisplay &
-r mli_driver3,quit -logfile junk.out >/dev/null",wait=.true.)
!!!!!!!!!!! Read wall and pressure profiles and qtank time history
open(file02,file='twall.txt')
do n=1,nlayer+2
    read(file02,*) twall(n)
enddo
close(file02)
open(file02,file='pgas.txt')
do n=1,nlayer
    read(file02,*) pgas(n)
```

```
enddo
close(file02)
open(file02,file='qtank.txt')
do n=1,nout
    read(file02,*) qtank(n)
enddo
close(file02)
end subroutine call_mli
```

REFERENCES

1. Vincenti, W.G.; and Krüger, Jr., C.H.: *Introduction to Physical Gas Dynamics*, John Wiley & Sons, New York, NY, p. 44, 1965.

2. Zucker, R.D.; and Biblarz, O.: *Fundamentals of Gas Dynamics*, John Wiley & Sons, New York, NY, p. 167, 1965.

3. Barron, R.F.: *Cryogenic Heat Transfer*, Taylor & Francis, Boca Raton, FL, p. 19, 1999.

4. Fesmire, J.E.; Johnson, W.L.; Meneghelli, B.J.; and Coffman, B.E.: "Cylindrical Boiloff Calorimeters for Testing of Thermal Insulation Systems," in *Advances in Cryogenic Engineering*: *Proceedings of the Cryogenic Engineering Conference* (*CEC*) *2015*, June 28–July 2, 2015, *IOP Conf. Series*: *Materials Science and Engineering*, Vol. 101, doi:10.1088/1757/899X, 2015.

5. Funke, T.; Golle, S.; and Haberstroh, C.: "Simulation of MLI Concerning the Influence of an Additional Heat Load on Intermediate Layers," *AIP Conference Proceedings*, Vol. 1573, p. 708, doi: 10.1063/1.4860772, 2014.

6. Martin, J.; and Hastings, L.: "Large-Scale Liquid Hydrogen Testing of a Variable Density Multilayer Insulation With a Foam Substrate," NASA/TM—2001–211089, NASA Marshall Space Flight Center, Huntsville, AL, 90 pp., June 2001.

7. Hasting, L.J.; Hedayat, A.; and Brown, T.M.: "Analytical Modeling and Test Correlation of Variable Density Multilayer Insulation for Cryogenic Storage," NASA/TM—2004–213175, NASA Marshall Space Flight Center, Huntsville, AL, 46 pp., May 2004.

REPORT DOCUMENTATION PAGE					*Form Approved OMB No. 0704-0188*
The public reporting burden for this collection of information is estimated to average 1 hour per response, including the time for reviewing instructions, searching existing data sources, gathering and maintaining the data needed, and completing and reviewing the collection of information. Send comments regarding this burden estimate or any other aspect of this collection of information, including suggestions for reducing this burden, to Department of Defense, Washington Headquarters Services, Directorate for Information Operation and Reports (0704-0188), 1215 Jefferson Davis Highway, Suite 1204, Arlington, VA 22202-4302. Respondents should be aware that notwithstanding any other provision of law, no person shall be subject to any penalty for failing to comply with a collection of information if it does not display a currently valid OMB control number. **PLEASE DO NOT RETURN YOUR FORM TO THE ABOVE ADDRESS.**					
1. REPORT DATE *(DD-MM-YYYY)* 01–12–2017		**2. REPORT TYPE** Technical Memorandum			**3. DATES COVERED** *(From - To)*
4. TITLE AND SUBTITLE Multilayer Insulation Ascent Venting Model					**5a. CONTRACT NUMBER**
					5b. GRANT NUMBER
					5c. PROGRAM ELEMENT NUMBER
6. AUTHOR(S) R.W. Tramel,* S.G. Sutherlin, and W.L. Johnson**					**5d. PROJECT NUMBER**
					5e. TASK NUMBER
					5f. WORK UNIT NUMBER
7. PERFORMING ORGANIZATION NAME(S) AND ADDRESS(ES) George C. Marshall Space Flight Center Huntsville, AL 35812					**8. PERFORMING ORGANIZATION REPORT NUMBER** M–1447
9. SPONSORING/MONITORING AGENCY NAME(S) AND ADDRESS(ES) National Aeronautics and Space Administration Washington, DC 20546–0001					**10. SPONSORING/MONITOR'S ACRONYM(S)** NASA
					11. SPONSORING/MONITORING REPORT NUMBER NASA/TM—2017–219844
12. DISTRIBUTION/AVAILABILITY STATEMENT Unclassified-Unlimited Subject Category 20 Availability: NASA STI Information Desk (757–864–9658)					
13. SUPPLEMENTARY NOTES Prepared by the Advanced Concepts Office, Engineering Directorate *Kord Technologies, Inc., Huntsville, AL **NASA Glenn Research Center, Cleveland, OH					
14. ABSTRACT The thermal and venting transient experienced by tank-applied multilayer insulation (MLI) in the Earth-to-orbit environment is very dynamic and not well characterized. This new predictive code is a first principles-based engineering model which tracks the time history of the mass and temperature (internal energy) of the gas in each MLI layer. A continuum-based model is used for early portions of the trajectory while a kinetic theory-based model is used for the later portions of the trajectory, and the models are blended based on a reference mean free path. This new capability should improve understanding of the Earth-to-orbit transient and enable better insulation system designs for in-space cryogenic propellant systems.					
15. SUBJECT TERMS cryogenic multi-layer insulation, cryogenic propellant storage, launch and ascent cryogenic fluid management, cryogenic insulation performance					
16. SECURITY CLASSIFICATION OF:			**17. LIMITATION OF ABSTRACT**	**18. NUMBER OF PAGES**	**19a. NAME OF RESPONSIBLE PERSON** STI Help Desk at email: help@sti.nasa.gov
a. REPORT U	**b. ABSTRACT** U	**c. THIS PAGE** U	UU	44	**19b. TELEPHONE NUMBER** *(Include area code)* STI Help Desk at: 757–864–9658

National Aeronautics and
Space Administration
IS02
George C. Marshall Space Flight Center
Huntsville, Alabama 35812